

The Effect of Rotation on The Boundary Layer Separation

Lazhar Bouchaour¹, Samia Benattalah²

¹ PhD student, Department of Physic Laboratory of Physic Energetic Frères Mentouri Constantine 1 University, Constantine, Algeria, email: lazharbouchaour@gmail.com

² Prof, Department of Physic Laboratory of Physic Energetic Frères Mentouri Constantine 1 University, Constantine, Algeria, email: s.benattalah@gmail.com

ARTICLE INFO

ABSTRACT

Received: 18 Dec 2024

Revised: 10 Feb 2025

Accepted: 28 Feb 2025

In this study, flow control on a NACA 0012 airfoil is investigated under various rotational speeds at a Reynolds number of $Re = 3.6 \times 10^5$. The commercial computational fluid dynamics (CFD) software, ANSYS Fluent, is utilized to perform the simulations. Both rotating and non-rotating cases are examined at a fixed angle of attack of 18° to assess the effects of rotation on aerodynamic performance

To analyze the stall-delay phenomenon in rotating airfoils, a combination of boundary layer theory, numerical simulations, and experimental measurements is employed. The results indicate that rotation significantly influences the flow behavior by delaying the onset of flow separation compared to the stationary (non-rotating) two-dimensional case. This rotational effect contributes to improved aerodynamic stability and lift characteristics, highlighting the potential of rotational motion as a passive flow control method for enhancing airfoil performance in relevant engineering applications.

Keywords: Cfd, Rotating Airfoil, Numerical Simulation , Separation , Rotational Effects

INTRODUCTION

On a rotating blade there's two main forces play an important role in separated boundary layer, i.e. the centrifugal forces that produce a span wise pumping effect that leads to the deviation of the streamlines in span wise direction towards to the tip. On the other hand, Coriolis force, which acts in the chord wise direction as a favorable pressure gradient that tends to delay separation [1].

Presently, rotational influences remain incompletely characterized and understood. The widely cited experiments of Himmelskamp indicate that stall delay and lift enhancement due to rotation were first noted for aircraft propellers. To explain these results, radial thinning and chordwise acceleration of the steady boundary layer, due to centrifugal forces and Coriolis effect, were postulated [2-4]. The effects of rotation on the boundary layer of a wind turbine blade have been found in many theoretical computations and experimental measurement data. During the last decades, researchers have studied the boundary layer development on a rotor, and several papers have been published about laminar boundary layer in a rotating condition. Of them, the most interesting one was a short technical note published by Banks and Gadd.

In this paper the authors assumed an external velocity with a linear adverse velocity gradient. They found that the separation point was postponed due to rotation, and for the extreme inboard stations the boundary layer was completely stabilized against separation[5].

The present work aims at giving a better understanding of the main influence of rotational effects on the boundary layer that develops over wind turbine blades.

Several studies in the past have been conducted to try to understand stall delay phenomenon for which no convincing and consistent physical description has been established yet. A 3d panel analysis of a HAWT was performed by Wood (1991) He found that when stall approached ,the large negative pressure gradients near the leading edge of a

rotating airfoil were reduced in magnitude as a result, the boundary layer separation was delayed on the suction surface due to this reduction of the adverse pressure gradient [6-7].

Recently, with the advent of the supercomputer, CFD tools have been employed to investigate this phenomenon. Narramore and Vermeland used a full Navier–Stokes equation solver with an algebraic turbulence model to calculate the flowfields on a high angle of attack on a helicopter rotor. The calculations showed that the separation point is delayed because of the effects of the rotation. They pointed out that the stall-delay effect is particularly pronounced for the inboard sections [8].

The Coriolis forces occurring in the boundary-layer flow are the main cause for the stall delay and increased three-dimensional post stall lift coefficients. Dimitrescu and Cardos (2004) and disagreed with the explanation provided by wood (1991) that stall delay was due to the external pressure gradient however Wood (2005) rebutted that the coriolis force whithin the boundary layer might not be the only mechanism for stall delay since Dumitrescu and Cardos (2004) did not consider the modifications to the external inviscid flow by the rotational effect [9].

Shen and Sorensen (1999) showed that the effect of rotation is to stabilize vortex shedding and suppress the growth of the separation bubble. Results from another navier- stokes modeling performed by Chaviaropoulos and Hansen (2000) revealed that when flow was massively separated at high AOA, the coriolis force redirected the flow within the separation bubble to the radiale direction and thus reduced the volume of separated flow which in turn induced a pressure drop on the suction surface of the rotating blade [6].

Coriolis and centrifugal forces play important roles in 3D stall-delay,. The 3D rotation effects are essentially the consequences of the centrifugal acceleration causing radial flow in the boundary layer and Coriolis forces tending to accelerate the flow in the chordwise direction toward the trailing edge (a reduction in the adverse pressure gradient). Therefore, this delays the occurrence of separation to a point further downstream .

The separation location is mainly affected by three key non-dimensional parameters (r/c , $\Omega r/U_\infty$, Re). The analysis shows that increasing $\Omega r/U_\infty$ and Re and decreasing r/c can result in the delay of the separation point[10].

MATHEMATICAL MODEL

Compared to wind tunnel measurements and airfoil computations the characteristics for airfoil sections on wind turbine blades are influenced by rotation and 3D flow. Since 2D computations give a fast way to obtain the characteristics, it is desirable to take account for rotational and 3D effects in computations on airfoil sections described in 2D airfoil computations [11]. The first attempt at calculating the boundary layer on a rotating blade was made by Fogarty in 1951 for the case of hovering flight. Fogarty made use of a theorem of Sears which states that if $\Phi_1(x, z)$ is the potential for plane steady flow past the cylinder in a parallel stream at unit speed, then the potential Φ for flow about the cylinder when rotating at angular velocity Ω is:

$$\Phi = \Omega [\Phi_1(x, z) - x] \tag{1}$$

It was also shown that the velocity components u_1 , v_1 , w_1 , relative to the blade are, Fig. 1

$$U_1 = \Omega y \frac{\partial \Phi_1}{\partial x} \tag{2}$$

$$V_1 = \Omega [\Phi_1(x, z) - 2x] \tag{3}$$

$$W_1 = \Omega y \frac{\partial \Phi_1}{\partial z} \tag{4}$$

Thus the velocity components u_1 and w_1 in the plane of the cylinder are the same as those of steady plane flow about the cylinder in a stream of velocity Ωy . The spanwise component v_1 , which is independent of the radial distance, can be found directly from the plane flow potential Φ_1 . These relationships establish the appropriate boundary conditions outside the boundary layer.

The equations used are the familiar Navier–Stokes equations referred to co-ordinates rotating with the blade, Fig 1. If the usual boundary layer approximations are made, and certain terms are neglected on account of the high aspect ratio of the blade, we have for the boundary layer equations [12].

$$u \frac{\partial u}{\partial x} + w \frac{\partial u}{\partial z} - \Omega^2 x = -\frac{1}{\rho} \frac{\partial p}{\partial x} + \nu \frac{\partial^2 u}{\partial z^2} \tag{5}$$

$$u \frac{\partial v}{\partial x} + w \frac{\partial v}{\partial z} - 2\Omega u - \Omega^2 y = -\frac{1}{\rho} \frac{\partial p}{\partial y} + \nu \frac{\partial^2 v}{\partial z^2} \tag{6}$$

$$\frac{\partial p}{\partial z} = 0 \tag{7}$$

Together with the continuity equation:

$$\frac{\partial u}{\partial x} + \frac{\partial w}{\partial z} = 0 \tag{8}$$

To find the pressure gradients $\frac{\partial p}{\partial x}$ and $\frac{\partial p}{\partial y}$ we use Bernoulli’s equation for the external potential flow, i.e

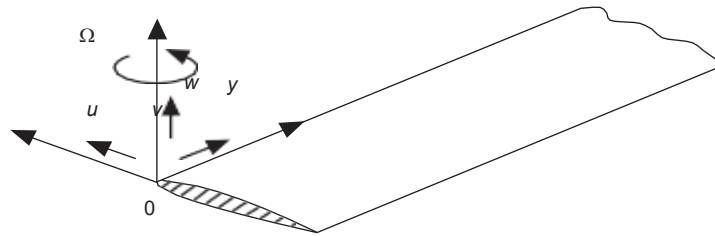


Figure 1. Rotating Blade

$$\frac{p}{\rho} + \frac{1}{2}(u_1^2 + v_1^2) = \frac{1}{2}\Omega^2(x^2 + y^2) + constant \tag{9}$$

Then, neglecting the small terms and $v_1 \frac{\partial v_1}{\partial y}$, we have approximately

$$\frac{1}{\rho} \frac{\partial p}{\partial x} = \Omega^2 x - u_1 \frac{\partial u_1}{\partial x} \tag{10}$$

$$\frac{1}{\rho} \frac{\partial p}{\partial y} = \Omega^2 y - u_1 \frac{\partial u_1}{\partial y} \tag{11}$$

So that, on substituting for the pressure gradients, the boundary layer equations are

$$u \frac{\partial u}{\partial x} + w \frac{\partial u}{\partial z} = u_1 \frac{\partial u_1}{\partial x} + \nu \frac{\partial^2 u}{\partial z^2} \tag{12}$$

$$u \frac{\partial v}{\partial x} + w \frac{\partial v}{\partial z} + 2\Omega u = u_1 \frac{\partial u_1}{\partial y} + \nu \frac{\partial^2 v}{\partial z^2} \tag{13}$$

$$\frac{\partial u}{\partial x} + \frac{\partial w}{\partial z} = 0 \tag{14}$$

Together with the boundary conditions

$$u = v = w = 0 \text{ for } z = 0$$

$$u \rightarrow U_1 = \Omega y \frac{\partial \Phi_1}{\partial x} \tag{15}$$

$$v \rightarrow v_1 = \Omega [\Phi_1(x, z) - 2x] \tag{16}$$

$$w \rightarrow W_1 = \Omega y \frac{\partial \Phi_1}{\partial z} \text{ for } z \rightarrow \infty \tag{17}$$

We notice that eq 12 is the same as the boundary layer equation for two-dimensional plane flow and may therefore be solved by any of the known methods. Having solved this equation for u and w , we can obtain v from the solution of eq 13. This has been done by Fogarty for the case of a flat plate and the section defined by $z = kx(1 - x^2)$.

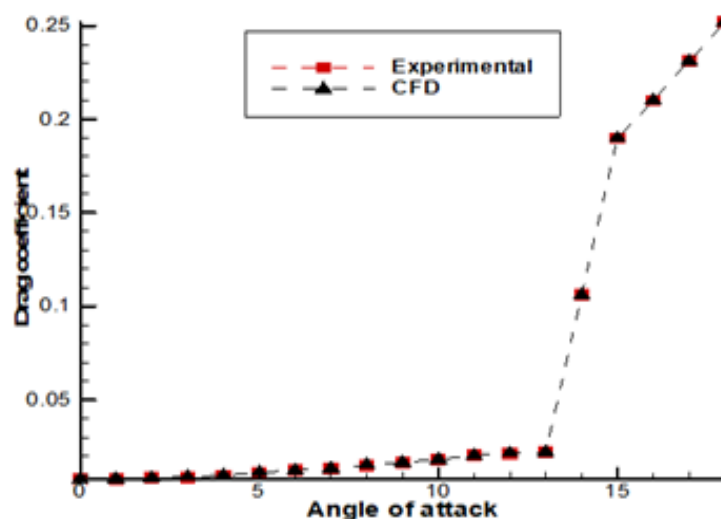
The significance of rotational forces on rotating blade aerodynamics first became apparent in 1947 with Himmelskamp’s investigations on the aerodynamic characteristics of propeller blade sections and the comparison to data obtained in a stationary reference frame. He found that rotation postpones stall onset to higher lift coefficients than it would be expected from non-rotating, two-dimensional tests with the same airfoil [13]

COMPUTATIONAL METHOD

The NACA 0012 airfoil, a well-characterized profile from the NACA 4-digit series, was selected due to its extensive documentation and widespread use in aerodynamic studies.

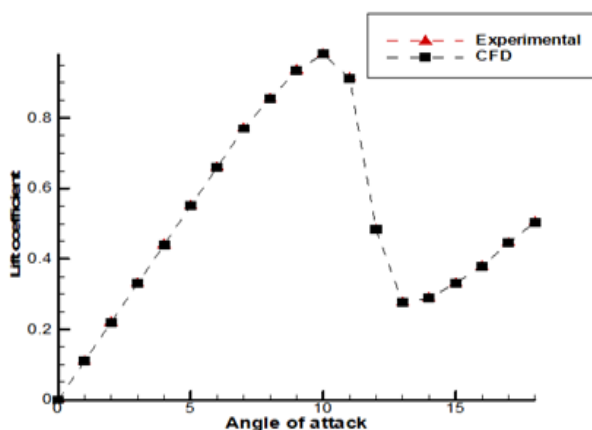
The Reynolds number for simulations expected from non-rotating two-dimensional tests with the same airfoil was set to approximately 3.6×10^5 . The computational model is tested for steady flow and the $k-\omega$ SST turbulence model has been used for turbulent computations, and then validate them with existing experimental data from reliable sources. To do so, the model was solved with a range of different angles of attack from 0 to 18° .

Fig 2 shows the lift and drag coefficients as a function of the angle of attack for the NACA 0012 airfoil, a commonly used airfoil in VAWTs, a comparison between the numerical study and the experimental results of Sheldahl and Klimas (1981) [14] is presented. This comparison gives a good agreement between the two results.



(a)

Figure 2. a Comparison between experimental and numerical results for NACA0012 aerofoil at a Reynolds number of 3.6×10^5 . Model Validation Study Drag Coefficient



(b)

Figure 2.b Comparison between experimental and numerical results for NACA0012 aerofoil at a Reynolds number of 3.6×10^5 . Model Validation Study Lift Coefficient

RESULTS AND DISCUSSION

After the validation a Simulations for various rotational speed were done in order to be able to compare the results from the rotating models and non-rotating naca 0012 airfoil.

The unsteady k- ω SST turbulence model has been used for turbulent computations at rotating speed of 120~300 rpm.

The effects of rotation on boundary layers separation are investigated.it is concluded that the height of the separated region is smaller for the rotating case than for the non-rotating case. This reduced height continues until rotational speed equal to 300 rpm. this is confirmed by Fig. 6 [15].

The streamlines around the rotating and non-rotating naca 0012 airfoil section are represented, Figure 3.2 shows the streamlines of non-rotating naca 0012 airfoil suction. The results show that at the angle of attack of 18 degrees we have separated flow on the clean airfoil. But In the case of rotating airfoil the flow is completely reattached at rotational speed equal to 300 rpm (figure 6.2). It is seen that the effect of rotation was to stabilize vortex shedding and suppress the growth of the separation bubble.

A similar conclusion was obtained in experimental research [11] [15].

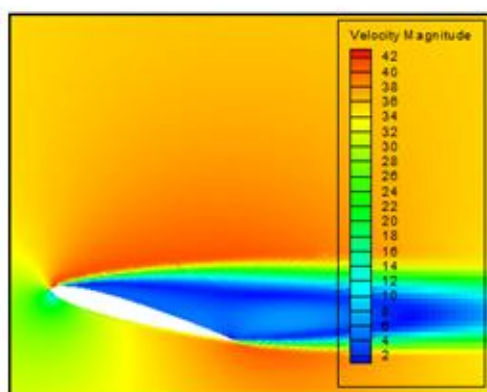


Figure. 3.1. Contour of velocity profile at AOA $\alpha= 18$ deg and $Re=3.6 \times 10^5$ the minimum and maximum values of the colour legend are mentioned below the figure.

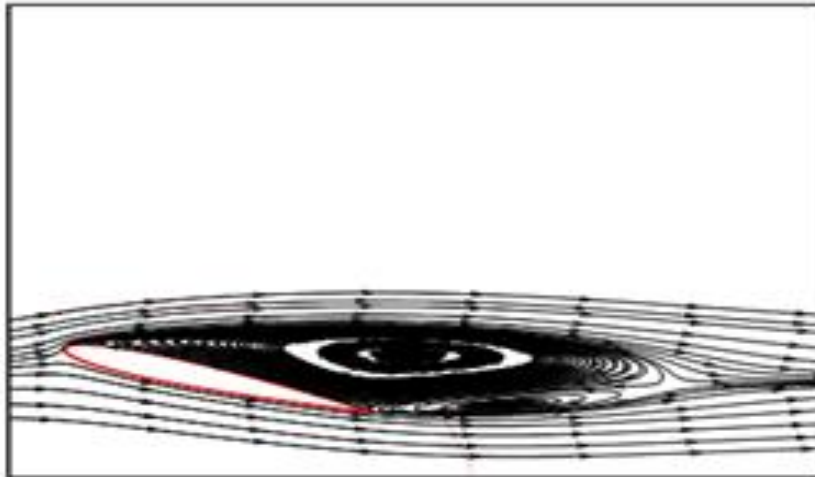


Fig. 3.2. Contour of streamline at angle of attack $\alpha=18$ and $Re=3.6 \times 10^5$

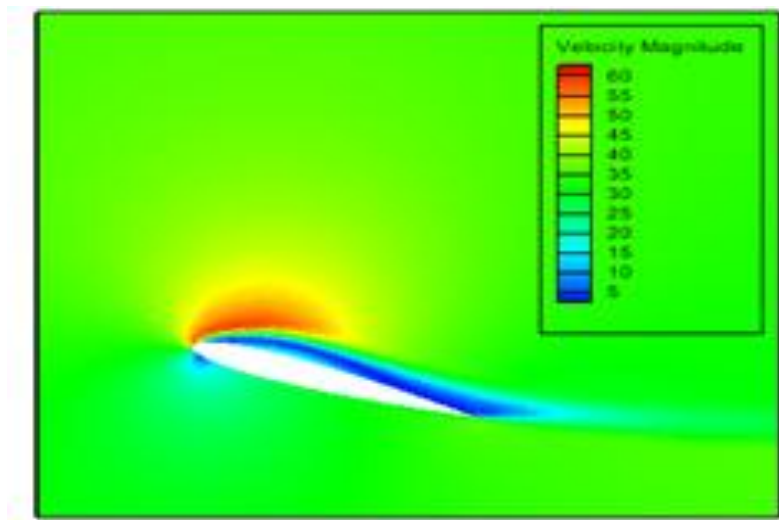


Figure. 4.1. Contour of velocity profile at angle of attack $\alpha=18$, $Re=3.6 \times 10^5$ and Rotational Speed = 120 rpm

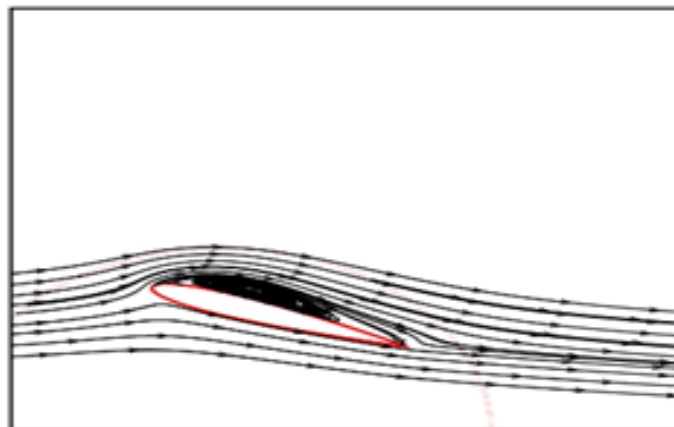


Figure. 4.2. Contour of stream line at angle of attack $\alpha=18$, $Re=3.6 \times 10^5$ and Rotational Speed = 120 rpm

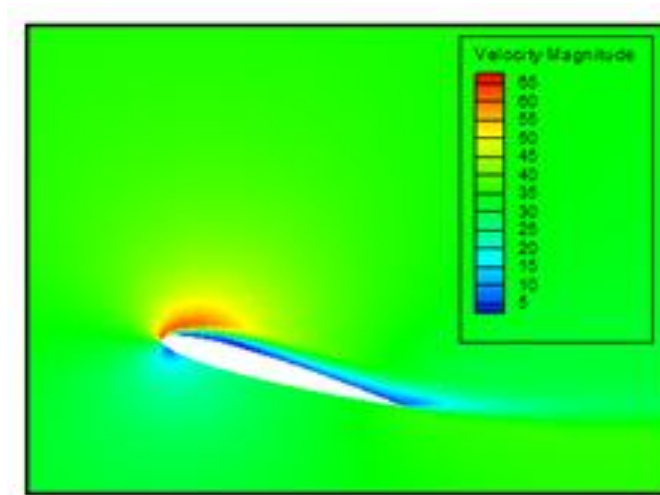


Figure. 5.1 Contour of velocity profile at angle of attack $\alpha= 18$, $Re=3.6 \times 10^5$ and Rotational Speed = 200 rpm

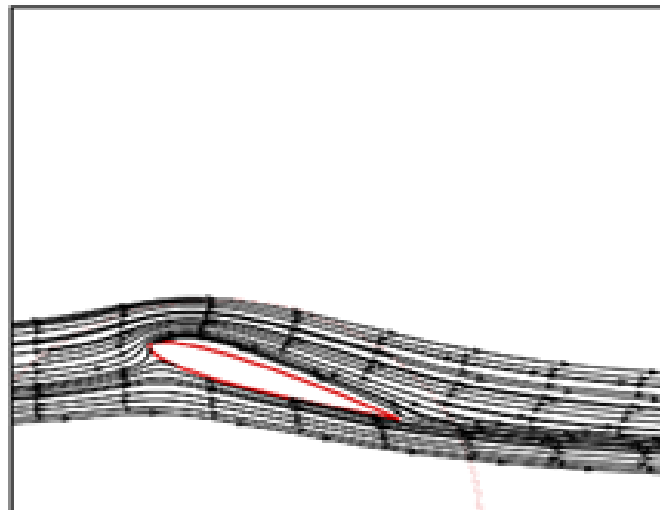


Figure. 5.2. Contour of stream line at angle of attack $\alpha=18$, $Re=3.6 \times 10^5$ and Rotational Speed = 200 rpm

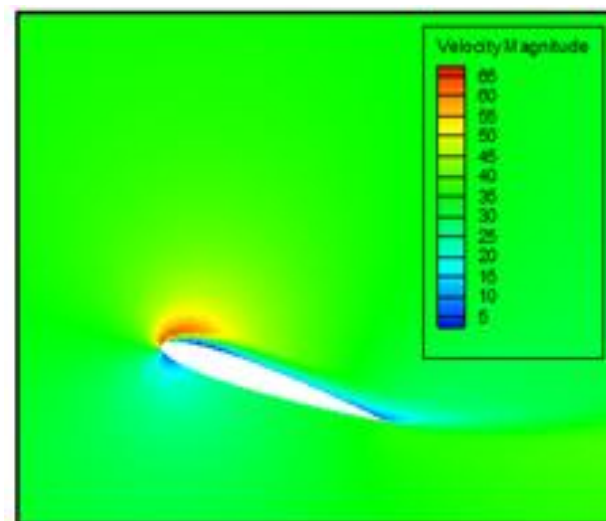


Figure. 6.1. Contour of velocity profile at angle of attack $\alpha=18$, $Re=3.6 \times 10^5$ and Rotational Speed = 300 rpm

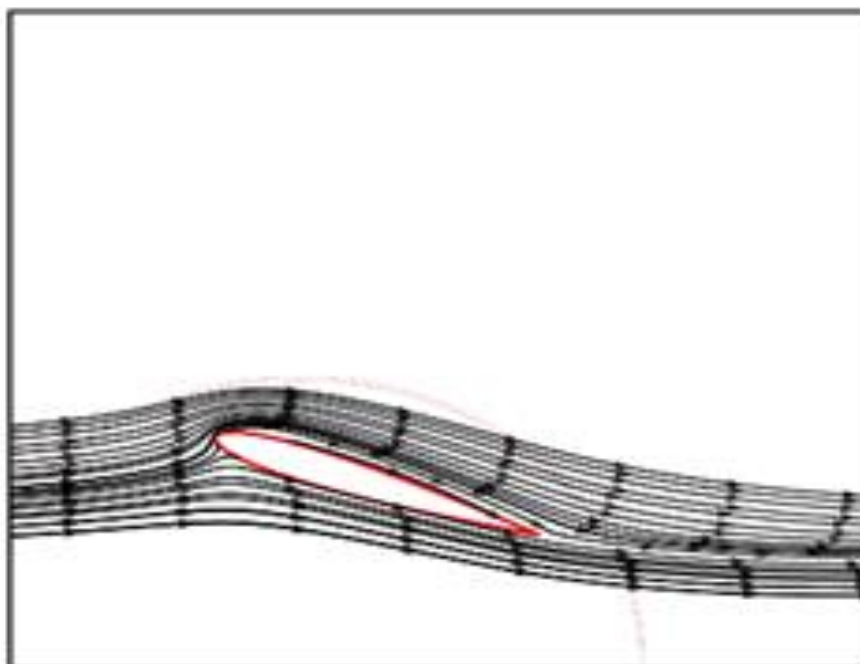


Figure. 6.2. Contour of stream line at angle of attack $\alpha=18$, $Re=3.6 \times 10^5$ and Rotational Speed = 300 rpm

CONCLUSIONS

The present study systematically investigates the boundary layer behavior of the NACA 0012 airfoil with the aim of controlling flow separation. As an initial step, a validation study is conducted using steady-state experimental data of lift and drag coefficients provided by Sheldahl and Klimas (1981) [14] at a Reynolds number of 3.6×10^5 . This comparison ensures the accuracy and reliability of the numerical methodology adopted in the current research.

Following validation, detailed computational simulations are performed using a commercial CFD code to analyze the flow field under two distinct conditions: a two-dimensional stationary airfoil and a two-dimensional rotating airfoil. The numerical results reveal that rotation significantly affects the development and separation of the boundary layer. Specifically, the centrifugal and Coriolis forces induced by rotation contribute to the delay of flow separation, thereby enhancing aerodynamic performance compared to the stationary case. These findings underscore the importance of rotational effects as a mechanism for passive flow control in aerodynamic applications.

REFERENCES

- [1] Riyadh Belamadi , Ramzi Mdouki, Adrian Ilinca and Abdelouaheb Djemili CFD study of a horizontal axis wind turbine NREL Phase II Revue des Energies Renouvelables Vol. 18 N°4 (2015) 683 – 700 Fields Wind Energ. 2007
- [2] Scott J. Schreck Rotationally Augmented Flow Structures and Time Varying Loads on Turbine Blades AIAA Aerospace Sciences Meeting and Exhibit 8 - 11 January 2007,
- [3] Scott J. Schreck, Niels N. Sørensen, Michael C. Robinson Aerodynamic Structures and Processes in Rotationally Augmented Flow Fields Wind Energ. 2007.
- [4] Horia Dumitrescu ,Maria Alexandrescu , Nicusor Alexandrescu Boudary Layer State And Flow Field Structure On Wind Turbine Blades Proceedings of the Romanian Academy, 2005
- [5] Zhaohui Du, Selig MS. The effect of rotation on the boundary layer of a wind turbine blade. J Renew Energy 2000;20(2):167–81
- [6] Hsiao Mun Lee, Yanhua Wu An experimental study of stall delay on the blade of a horizontal-axis wind turbine using tomographic particle image velocimetry J. Wind Eng. Ind. Aerodyn. 123 (2013) 56–68
- [7] Wood DH. Three-dimensional analysis of stall-delay on a horizontal-axis wind turbine. J Wind Eng Ind Aerodyn 1991;37:1–14.

- [8] Danmei Hu, Ouyang Hua, Zhaohui Du. A study on stall-delay for horizontal axis wind turbine Renewable Energy 31 (2006) 821–836
- [9] Horia Dumitrescu and Vladimir Cardos Rotational Effects on the Boundary-Layer Flow in Wind Turbines AIAA JOURNAL, VOL. 42, NO. 2. <https://doi.org/10.2514/1.9103>
- [10] N.Tenguria, N.D. Mittal, S.Ahmed Review on Horizontal Axis Wind Turbine Rotor Design and Optimization Trends in applied Sciences Research 6 (2011)
- [11] Bak, C., Fuglsang, P., Sørensen, N. N., Aagaard Madsen, H., Shen, W. Z., & Sørensen, J. N. Airfoil characteristics for wind turbines. Denmark. Forskningscenter Risoe. Risoe-R No. 1065(EN) (1999)
- [12] George Done, David Balmford. Bramwell, A. R. S. Bramwell's helicopter dynamics 2nd ed. Oxford: Butterworth- Heinemann, 2001.
- [13] Von Armin Weiss, M.Sc. investigations of boundary-layer transition and airloads on rotating blades doctorat thesis 2018
- [14] Sheldal, R. E., Klimas, P. C., Aerodynamic characteristics of Seven symmetrical airfoil sections through 180-degree angle of attack for use in aerodynamic analysis of vertical axis wind turbines. 1980. SAND 80-2114
- [15] Wen Zhong Shen and Jens Nørkær Sørensen, Quasi-3D Navier–Stokes Model for a Rotating Airfoil. 1980. Journal of Computational Physics 150, 518–548 (1999)